

# Neoclassical Growth Model with Two Fixed Delays\*

Luca Guerrini<sup>†</sup> Akio Matsumoto<sup>‡</sup> Ferenc Szidarovszky<sup>§</sup>

## Abstract

"Delay" has been considered as one of destabilizing factors in economic dynamics since the seminal work of Kalecki (1935). Dynamic macroeconomic is concerned with explaining growth and fluctuations. This paper shows how various dynamics involving cyclic fluctuations can emerge in the standard neoclassical growth model when two distinct delays, a delay in production and a delay in depreciation, are explicitly taken into account. We first confirm that the production delay has a stabilizing effect and the depreciation delay has a destabilizing effect in a one-delay model. We then analytically derive the conditions for which stability is lost and the bifurcates to a cycle via Hopf bifurcation. The Cobb-Douglas production function is adopted to illustrate the analytical result numerically. It is found that stability loss and gain repeatedly occur in the two delay model. This implies that the delay is not only a destabilizer but also a stabilizer. On a technical level, we have a stability switching curves that are obtained by applying a two delay differential equation.

**Keywords:** Two fixed delays, Stability crossing curve, Hopf bifurcation, Neoclassical growth model

---

\*The authors thank two anonymous referees for helpful and constructive comments on earlier version of the paper. The second author highly acknowledges the financial supports from the Japan Society for the Promotion of Science (Grant-in-Aid for Scientific Research (C), 16K03556) and Chuo University (Joint Research Grant). The usual disclaimers apply.

<sup>†</sup>Department of Management, Polytechnic University of Marche, 60121 Ancona, Italy. luca.guerrini@univpm.it

<sup>‡</sup>Department of Economics, Chuo University, 742-1, Higashi-Nakano, Hachioji, Tokyo 192-0393, Japan. akiom@tamacc.chuo-u.ac.jp

<sup>§</sup>Department of Mathematics, Corvinus University, Budapest, Fővám tér, 1093, Hungary. szidarka@gmail.com

# 1 Introduction

For more than a half-century, the neoclassical growth model of Solow (1956) and Swan (1956) has been a prototype for analyzing long-run economic growth. It has the general equilibrium structure although very simple and it brings out how an economy can enjoy positive growth rates in a very clear way. The model is applied to study analytically as well as numerically topics including multisector growth, cross-country income difference, nonlinear population growth, the empirics of economic growth, etc. On the other hand, business cycles that are the main concern of macroeconomics are often observed in a real economy, however, the neoclassical model makes only limited contributions to explain such cyclic dynamics since its steady state is locally asymptotically stable, implying that its dynamics is monotonic or oscillatory convergent.

So far, there are several turning points at which its basic structure is modified so as to give rise to cyclical fluctuations. Among others, Day (1982) incorporates the two opposite effects of increasing capital stock into the neoclassical model, one is the positive effect that is an essential source of economic growth and the other is the negative effects caused by environmental distortion of high economic growth such as pollutions. It is then demonstrated in a discrete-time framework that persistent irregular fluctuations including chaos can be generated when nonlinearities due to the two effects get stronger. It is thus confirmed that a strong nonlinearity can be a source of cyclical behavior. Since the seminal work of Kalecki (1935), it has been conjectured that a production delay could be a source of economic fluctuations. Kydland and Prescott (1982) construct the equilibrium growth model and empirically confirm that a production delay is crucial for explaining aggregate fluctuation. Recently, Zak (1999) and Szydłowski and Krawiec (2004) introduce the Kaleckian production delay into the growth model and show an emergence of a cycle via a Hopf bifurcation. Matsumoto and Szidarovszky (2011) reconsider Day's discrete time model in a continuous-time framework with the production delay. The birth of chaotic dynamics through a period-doubling cascade is numerically verified. It conveys a new result that nonlinearities and production delays are responsible for the birth of chaotic dynamics in a continuous-time framework.

More recently, Bianca et al. (2013) extend analysis to the case in which the neoclassical model has two distinct delays, one refers to the time when capital is used for production and the other to the necessary time for the capital to be depreciated. By applying the normal theory and center manifold argument, they demonstrate the existence, the direction and stability of a Hopf bifurcation. They have taken some important steps to affirm the active roles of the delays. Further, their results can be improved more if we can construct analytical conditions for which the stationary point of the two delays growth model becomes stable or unstable. The main purpose of this study is to reconfirm and extend their results in more systematic way by applying the mathematical method developed by Gu et al. (2005) to deal with two delay models, through the use of the *stability switching curves*. We will look more carefully not only the production delay but also the delay in depreciation as sources for macroeconomic fluctuations.

The rest of the paper is organized as follows. Section 2 builds a one-delay growth model to discuss the Kaleckian production delay. Section 3 derives the complete form of the stability switching curve under two delays and determines the direction of crossing the imaginary axis. Section 4 confirms the analytical results numerically in our own example and reexamines two other examples provided by Bianca et al. (2013) in our way. Finally, concluding remarks are given in Section 4.

## 2 One delay growth model

In the literature, there are two different versions of a delay growth model. One displays a Kaleckian gestation delay in investment inherent in the production process and no delay in depreciation of the capital. Consequently, its capital stock accumulation is described by

$$\dot{k}(t) = sf(k(t - \tau)) - \delta k(t). \quad (1)$$

Here  $k(t)$  is the capital stock per capita at time  $t$  in continuous time,  $\tau > 0$  is the delay indicating that the capital installed at time  $t - \tau$  becomes available at time  $t$ ,  $s \in (0, 1)$  is a constant saving rate,  $\delta \in (0, 1]$  is the depreciation rate and  $f(k)$  is well-behaved neoclassical production function implying that it is continuous, increasing, strictly concave,  $f(0) = 0$  and satisfies Indada's conditions. The other characterizes the case in which the capital depreciation starts after the capital becomes productive,

$$\dot{k}(t) = sf(k(t - \tau)) - \delta k(t - \tau). \quad (2)$$

A lot of efforts have been devoted to study how the gestation delay affects dynamics. As will be seen shortly, the delay in (1) does not affect stability and the delay in (2) can destabilize it when the length of the delay becomes large enough. Comparing these results easily and reasonably leads us to mention that the delay in depreciation matters. However, studying effects caused by the depreciation delay has been limited. To shed light on roles of the depreciation delay in emergence of macro cyclic oscillations, we move one step forward and consider two different fixed delays,

$$\dot{k}(t) = sf(k(t - \tau_1)) - \delta k(t - \tau_2) \quad (3)$$

where we call  $\tau_1$  a gestation delay and  $\tau_2$  a depreciation delay henceforth. In doing so, we can investigate delay effects caused by a change in  $\tau_1$  or  $\tau_2$ .

We interpret the depreciation delay as an information collecting delay with the following reasons. Capital  $k(t)$  represents the durable physical units such as machines, buildings, factories and so on. Depreciation is thought to be a decrease in the economic value of the capital. Thus the capital will be depreciated through physical depreciation, obsolescence or changes in demand for its service. However, in real world, there are some difficulties in determining "depreciation" and "value" with sufficient accuracy. It is apparently challenging to measure physical depreciation of the capital while operating it. It is also difficult to predict future demand fluctuations instantaneously. On the other hand, the capital value is considered to be the present value of the flow of services the capital will generate in future. Hence, to determine the value, it is, at least, necessary to obtain information on the life of the capital and the scrap value at the end of the life. Again, to obtain the accurate values of these poses serious challenge. It is often observed that the exactly same two machines may have different life time and different scrap values under the different operational environments. Since many diverse factors affect those values, it may take some amount of time to evaluate correctly the capital value on which depreciation will be determined. Since the factors affecting the length of  $\tau_1$  and  $\tau_2$  are independent and interdependent, it is undetermined in general which has a longer length. If the depreciation is thought to start after the capital becomes productive,  $\tau_2$  could be longer than  $\tau_1$ . If the depreciation starts before capital is activated,  $\tau_2$  could be shorter. Our consideration reveals that the depreciation delay plays a positive role affecting economic fluctuations.

A stationary point of (3) is a positive solution of  $sf(k) - \delta k = 0$ , where existence and number of equilibria depend on properties of function  $f$ . To examine stability of an stationary point of (3), say  $k^*$ , (3) is linearized at  $k = k^*$ ,

$$\dot{k}(t) = s\alpha[k(t - \tau_1) - k^*] - \delta[k(t - \tau_2) - k^*], \quad (4)$$

where  $\alpha = f'(k^*)$  and  $s\alpha < \delta$  due to Inada's conditions. Looking for exponential solutions of homogeneous version of (4), that is solution of the form  $k(t) = e^{\lambda t}u$  with  $u$  a constant, then, after substitution, we obtain the corresponding characteristic equation

$$\lambda - s\alpha e^{-\lambda\tau_1} + \delta e^{-\lambda\tau_2} = 0. \quad (5)$$

In case of absence of delays, (5) becomes  $\lambda = s\alpha - \delta < 0$  and thus, the stationary point  $k^*$  of (3) is locally asymptotically stable.

Before proceeding to the general case where two delays are positive, we quickly overview the special case in which only one delay is positive in (5). There are three cases depending on which variable has a delay, (1)  $\tau_1 = 0$  and  $\tau_2 > 0$ , (2)  $\tau_1 > 0$  and  $\tau_2 = 0$  and (3)  $\tau_1 = \tau_2 = \tau > 0$ . For each of three, we have a corresponding result.

**Lemma 1** *If  $\tau_1 = 0$  and  $\tau_2 > 0$ , then there is a critical value  $\tau_2^* > 0$  such that the stationary state of equation (4) is locally asymptotically stable for  $\tau_2 < \tau_2^*$  and unstable for  $\tau_2 > \tau_2^*$  where*

$$\tau_2^* = \frac{\pi}{\sqrt{\delta^2 - (\alpha s)^2}} \sin^{-1} \left( \frac{\sqrt{\delta^2 - (\alpha s)^2}}{\delta} \right).$$

Furthermore, equation (4) undergoes a Hopf bifurcation at  $k^*$  when  $\tau_2 = \tau_2^*$ .

**Proof.** The characteristic equation (5) is reduced to

$$\lambda - s\alpha + \delta e^{-\lambda\tau_2} = 0.$$

Under the assumption of  $\lambda = i\omega$  with  $\omega > 0$ , separating the real and imaginary parts of the characteristic equation gives rise to

$$\delta \cos \omega\tau = \alpha s$$

$$\delta \sin \omega\tau = \omega.$$

Squaring both equations and adding them present

$$\omega^* = \sqrt{\delta^2 - (\alpha s)^2} > 0$$

Substituting  $\omega^*$  into the imaginary part,  $\delta \sin \omega\tau = \omega$ , and then solving for  $\tau$  yields the critical value  $\tau_2^*$  in the form given above.<sup>1</sup> Selecting  $\tau_2$  as the bifurcation parameter, we consider  $\lambda$  as function of  $\tau_2$ :  $\lambda = \lambda(\tau_2)$ . Differentiating the characteristic equation with respect to  $\tau_2$ , we obtain

$$[1 - (s\alpha - \lambda)\tau_2] \frac{d\lambda}{d\tau_2} = \lambda(s\alpha - \lambda).$$

It is immediate to check that  $i\omega^*$  is a simple root. In fact, if it were a repeated root, then  $\lambda = i\omega$  would satisfy both equations

$$\lambda - s\alpha + \delta e^{-\lambda\tau_2} = 0 \text{ and } 1 + \delta e^{-\lambda\tau_2} (-\tau_2) = 0$$

---

<sup>1</sup>Substituting  $\omega^*$  into the real part presents the same critical value in a different form.

implying that  $0 = 1 - \tau_2(s\alpha - \lambda)$ , which is impossible if  $\lambda$  is purely imaginary. Next, we have

$$\text{sign} \left[ \frac{d(\text{Re}\lambda)}{d\tau_2} \right]_{\lambda=i\omega^*, \tau_2=\tau_2^*} = \text{sign} \left[ \text{Re} \left( \frac{d\lambda}{d\tau_2} \right)^{-1} \right]_{\lambda=i\omega^*, \tau_2=\tau_2^*} = \text{sign} \left[ \frac{1}{(\omega^*)^2 + s^2\alpha^2} \right] > 0.$$

This inequality implies that all roots cross the imaginary axis at  $i\omega$  from left to right as  $\tau_2$  increase, which completes the proof. ■

**Lemma 2** *If  $\tau_1 > 0$  and  $\tau_2 = 0$ , then the stationary point of (4) is locally asymptotically stable for any value of  $\tau_1 > 0$ .*

**Proof.** We can prove this Lemma in the same way as Lemma 1. Indeed, the characteristic equation (5) is reduced to

$$\lambda + \delta - \alpha s e^{-\lambda\tau} = 0.$$

Assume that  $\lambda = i\omega$  with  $\omega > 0$  with which the real part and imaginary part of the characteristic equation are

$$s\alpha \cos \omega\tau = \delta$$

$$s\alpha \sin \omega\tau = -\omega.$$

Squaring both sides of each equation and adding them give

$$\omega^2 = (\alpha s)^2 - \delta^2 < 0$$

where the inequality is due to  $s\alpha < \delta$ . Hence there is no  $\omega$  satisfying the characteristic equation. No stability switch occurs. ■

**Lemma 3** *If  $\tau_1 = \tau_2 = \tau > 0$ , then there is a critical value  $\tau^*$  such that the stationary point is locally asymptotically stable for  $\tau < \tau^*$  and unstable for  $\tau > \tau^*$  where*

$$\tau^* = \frac{\pi}{2(\delta - \alpha s)} > 0.$$

**Proof.** The characteristic equation (5) is reduced to

$$\lambda + (\delta - s\alpha) e^{-\lambda\tau} = 0.$$

Assume that  $\lambda = i\omega$  with  $\omega > 0$ . It is substituted into the above characteristic equation that is separated to the real part and the imaginary part,

$$(\delta - s\alpha) \cos \omega\tau = 0$$

$$(\delta - s\alpha) \sin \omega\tau = \omega.$$

Both equations is solved simultaneously to obtain a solution of  $\omega$  denoted by  $\omega^*$ . We then have  $\omega^* \tau = \pi/2$  from the real part and  $\omega^* = \delta - s\alpha$  from the imaginary part. From the second equation above, we can obtain the value of  $\tau$  for which the characteristic equation has pure imaginary roots,

$$\tau^* = \frac{\pi}{2(\delta - \alpha s)}.$$

Hence we obtain stability for  $\tau < \tau^*$  and instability for  $\tau > \tau^*$ . ■

Lemma 1 is a new result that the depreciation delay can destabilize the stationary point, which is locally asymptotically stable otherwise. Lemma 2 is equivalent to Proposition 1 of Bianca et al. (2013) that the gestation delay is *harmless* or, it could be said, a stabilizer, meaning that stability of the stationary state is preserved regardless of values of  $\tau_1$ . Lemma 3 has been considered in Zak (1999)<sup>2</sup> and shows that a larger length of the equal delay can make the stationary point unstable. It is further possible to show that a stationary point of (4) bifurcates to a periodic cycle at the critical point  $\tau^*$  as shown in Lemma 1. In Lemmas 1 and 3, there are infinitely many solutions for  $\tau_2$  and  $\tau$ . We show that at all  $\tau_2$  and  $\tau$ , one eigenvalue changes real prt from negative to positive, and stability is lost at the smallest critical values of  $\tau_2$  and  $\tau$ .<sup>3</sup> These critical values of the delay indicate that as the lengths of delay change, the stability of the stationary point qualitatively changes. Such phenomena are referred to as *stability switch*.

In Figure 1, the stability switching loci of  $\tau^*$  and  $\tau_2^*$  are illustrated with respect to  $\delta$  as downward-sloping blue and red curves in which  $\alpha s$  is taken to be 1/10. It is seen that the blue curve is located above the red curve. This difference between  $\tau^*$  and  $\tau_2^*$  (that is, the striped region) is due to a stabilizing role of the gestation delay. On the red curve, the depreciation delay in equation (1) destabilizes the stationary point whereas, in equation (2), the stabilizing effect caused by the gestation delay dominates the destabilizing effect by the depreciation effect. Thus, equation (2) is still stable there. Hence Lemmas 1, 2 and 3 lead to the following result.

**Theorem 1** *A delay neoclassical growth model is always stable when it has only a gestation delay,  $\tau_1$  and becomes unstable when it has only a depreciation delay and  $\tau_2 > \tau_2^*$ . It is numerically verified that the stable region of the equal delay model is larger than that of the model with  $\tau_2$  due to the stabilizing effect of  $\tau_1$ .*

---

<sup>2</sup>However, his proof is inaccurate. His equations (6) and (7) corresponds to the imaginary and real parts but are different from ours although the characteristic equation is the same. " $\mu$ " in his (6) should be interchanged with " $\omega$ " in his (7).

<sup>3</sup>See Matsumoto and Szidarovszky (2012, 2013) for more rigorous discussions.

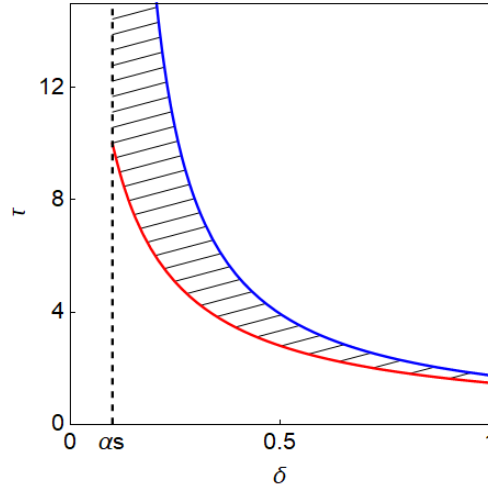


Figure 1. Stability switching curves,  $\tau^*$  and  $\tau_2^*$

### 3 Two Delay Growth Model

We now consider the general case of  $\tau_1 > 0$ ,  $\tau_2 > 0$  and  $\tau_1 \neq \tau_2$ , focusing on the stabilizing effect of  $\tau_1$  and the destabilizing effect of  $\tau_2$ . This issue has not been investigated yet and is the main part of this study. As  $\tau_1$  and  $\tau_2$  change, equation (3) can switch from stability to instability, or vice versa, only when at least one characteristic root moves to the imaginary axis. Thus, the stability analysis of (3) requires calculating the characteristic roots  $\lambda = i\omega$  of the characteristic equation (5). To study the change of stability when  $\tau_1$  and  $\tau_2$  both vary, we will follow the methodology of Gu et al. (2005) with the use of the stability crossing curves, which are defined as the curves that separate the stable and unstable regions in the  $(\tau_1, \tau_2)$  plane. To apply this method, we rewrite equation (5) as

$$p(\lambda, \tau_1, \tau_2) = p_0(\lambda) + p_1(\lambda)e^{-\lambda\tau_1} + p_2(\lambda)e^{-\lambda\tau_2} = 0, \quad (6)$$

where

$$p_0(\lambda) = \lambda, \quad p_1(\lambda) = -s\alpha, \quad p_2(\lambda) = \delta.$$

Next we check the following assumptions on  $p(\lambda, \tau_1, \tau_2)$  to exclude some obvious trivial cases:

- I)  $\deg[p_0(\lambda)] \geq \max\{\deg[p_1(\lambda)], \deg[p_2(\lambda)]\}$  (existence of a principal term).
- II)  $p_0(0) + p_1(0) + p_2(0) \neq 0$  ("0" is not a solution of (6) for any pair  $(\tau_1, \tau_2)$ ).
- III) The polynomials  $p_0(\lambda), p_1(\lambda)$  and  $p_2(\lambda)$  do not have common roots (in order to simplify the expressions).
- IV)  $\lim_{\lambda \rightarrow \infty} \left( \left| \frac{p_1(\lambda)}{p_0(\lambda)} \right| + \left| \frac{p_2(\lambda)}{p_0(\lambda)} \right| \right) < 1$  (restriction on difference operator).

Now, conditions I), II) and IV) hold since  $\deg[p_0(\lambda)] = 1$  and  $\deg[p_1(\lambda)] = \deg[p_2(\lambda)] = 0$ ,  $p_0(0) + p_1(0) + p_2(0) = -s\alpha + \delta \neq 0$ , and the limit of each fraction in absolute value is equal to zero as  $\lambda \rightarrow \infty$ , respectively. Finally, condition III) is clearly satisfied.

A pair  $(\tau_1, \tau_2) \in R_+^2$  is said to be a crossing point if  $p(\lambda, \tau_1, \tau_2) = 0$  has at least one solution for  $\lambda$  on the imaginary axis. The set of all crossing points is known as the stability crossing set, and is denoted by  $T$ . An  $\omega > 0$  is known as a crossing frequency if there exists at least one pair  $(\tau_1, \tau_2)$  such that  $p(i\omega, \tau_1, \tau_2) = 0$ . The set  $\Omega$  of all crossing frequencies is called the crossing frequency set, i.e.,

$$\Omega = \{\omega > 0 : p(i\omega, \tau_1, \tau_2) = 0 \text{ for some } (\tau_1, \tau_2) \in R_+^2\}$$

Considering that  $p_0(\lambda)$  has no nonzero roots on the imaginary axis, the stability analysis of (6) can be reduced to the analysis of the equation

$$a(\lambda, \tau_1, \tau_2) = 1 + a_1(\lambda)e^{-\lambda\tau_1} + a_2(\lambda)e^{-\lambda\tau_2} = 0, \quad (7)$$

where

$$a_1(\lambda) = \frac{p_1(\lambda)}{p_0(\lambda)} = -\frac{s\alpha}{\lambda}, \quad a_2(\lambda) = \frac{p_2(\lambda)}{p_0(\lambda)} = \frac{\delta}{\lambda}.$$

The form of equation (7) allows to replace the investigation on crossing the imaginary axis into the geometric problem of a triangle. Specifically, for each given  $\lambda = i\omega$ ,  $\omega > 0$ , the term  $a(\lambda, \tau_1, \tau_2)$  is represented in the complex plane as the sum of three vectors 1,  $a_1(\lambda)e^{-\lambda\tau_1}$  and  $a_2(\lambda)e^{-\lambda\tau_2}$ , with magnitudes 1,  $|a_1(i\omega)|$  and  $|a_2(i\omega)|$ , respectively, which are independent of  $\tau_1$  and  $\tau_2$ . If these vectors create a triangle (i.e.,  $a(\lambda, \tau_1, \tau_2) = 0$ ), then the characteristic equation has a solution  $\lambda = i\omega$  for some delays  $\tau_1$  and  $\tau_2$ . Since the length of each edge of a triangle cannot exceed the sum of the lengths of the remaining two edges, we derive that the range of  $\omega$  to parameterize  $T$  are the solution of the following three inequalities:

$$|a_1(i\omega)| + |a_2(i\omega)| \geq 1, \quad -1 \leq |a_1(i\omega)| - |a_2(i\omega)| \leq 1. \quad (8)$$

Since

$$|a_1(i\omega)| = \left| -\frac{s\alpha}{i\omega} \right| = \frac{s\alpha}{\omega} \quad \text{and} \quad |a_2(i\omega)| = \left| \frac{\delta}{i\omega} \right| = \frac{\delta}{\omega},$$

the triangle conditions (8) give

$$s\alpha + \delta \geq \omega, \quad -\omega \leq s\alpha - \delta \leq \omega.$$

Recalling  $s\alpha - \delta < 0$ , we obtain

$$-s\alpha + \delta \leq \omega \leq s\alpha + \delta. \quad (9)$$

As a result, we get

$$\Omega = [-s\alpha + \delta, s\alpha + \delta].$$

For any  $\omega \in \Omega$ , the characteristic equation (4) has a pair of purely imaginary roots and it is now possible to identify solutions  $(\tau_1, \tau_2)$  of  $p(\lambda, \tau_1, \tau_2) = 0$  as the following two sets of curves in the first quadrant of the  $(\tau_1, \tau_2)$ -region:

$$C^+(m, n) : \begin{cases} \tau_{1,m}^+ = \tau_{1,m}^+(\omega) = \frac{\arg[a_1(i\omega)] + (2m-1)\pi + \theta_1(\omega)}{\omega} \\ \tau_{2,n}^+ = \tau_{2,n}^+(\omega) = \frac{\arg[a_2(i\omega)] + (2n-1)\pi - \theta_2(\omega)}{\omega} \end{cases} \quad (10)$$



and

$$C^-(m, n) : \begin{cases} \tau_{1,m}^- = \tau_{1,m}^-(\omega) = \frac{\arg[a_1(i\omega)] + (2m-1)\pi - \theta_1(\omega)}{\omega} \\ \tau_{2,n}^- = \tau_{2,n}^-(\omega) = \frac{\arg[a_2(i\omega)] + (2n-1)\pi + \theta_2(\omega)}{\omega} \end{cases} \quad (11)$$

for  $m = m_0^\pm, m_0^\pm + 1, m_0^\pm + 2, \dots$ , and  $n = n_0^\pm, n_0^\pm + 1, n_0^\pm + 2, \dots$ , where  $n_0^+, n_0^-, m_0^+, m_0^-$  ( $n_0^+ \leq n_0^-$  and  $m_0^+ \geq m_0^-$ ) are the smallest possible integers such that the corresponding  $\tau_1^{n_0^+}, \tau_1^{n_0^-}, \tau_2^{m_0^+}, \tau_2^{m_0^-}$  values are nonnegative.

In the expressions (10) and (11), the terms  $\arg[a_1(i\omega)]$  and  $\arg[a_2(i\omega)]$  denote the argument of  $a_1(i\omega)$  and  $a_2(i\omega)$ , respectively, and are given by

$$\arg[a_1(i\omega)] = \arg\left[-\frac{s\alpha}{i\omega}\right] = \arg\left[\frac{s\alpha}{\omega}i\right] = \frac{\pi}{2}$$

and

$$\arg[a_2(i\omega)] = \arg\left[\frac{\delta}{i\omega}\right] = \arg\left[-\frac{\delta}{\omega}i\right] = \frac{3\pi}{2},$$

while  $\theta_1, \theta_2 \in [0, \pi]$  represent the internal angles of the triangle, and are determined by the law of cosines as follows,

$$\theta_1(\omega) = \cos^{-1}\left(\frac{1 + |a_1(i\omega)|^2 - |a_2(i\omega)|^2}{2|a_1(i\omega)|}\right) = \cos^{-1}\left(\frac{\omega^2 + s^2\alpha^2 - \delta^2}{2s\alpha\omega}\right)$$

and

$$\theta_2(\omega) = \cos^{-1}\left(\frac{1 + |a_2(i\omega)|^2 - |a_1(i\omega)|^2}{2|a_2(i\omega)|}\right) = \cos^{-1}\left(\frac{\omega^2 - s^2\alpha^2 + \delta^2}{2\delta\omega}\right).$$

The inequalities in (9) yield that the arccosine functions are well-defined being

$$-1 \leq \frac{\omega^2 + s^2\alpha^2 - \delta^2}{2s\alpha\omega} \leq 1 \quad \text{and} \quad -1 \leq \frac{\omega^2 - s^2\alpha^2 + \delta^2}{2\delta\omega} \leq 1.$$

In conclusion, equations (10) and (11) are given by

$$C^+(m, n) : \begin{cases} \tau_{1,m}^+(\omega) = \frac{1}{\omega} \left[ -\frac{\pi}{2} + 2m\pi + \cos^{-1}(A) \right] \\ \tau_{2,n}^+(\omega) = \frac{1}{\omega} \left[ \frac{\pi}{2} + 2n\pi - \cos^{-1}(B) \right] \end{cases} \quad (12)$$

and

$$C^-(m, n) : \begin{cases} \tau_{1,m}^-(\omega) = \frac{1}{\omega} \left[ -\frac{\pi}{2} + 2m\pi - \cos^{-1}(A) \right] \\ \tau_{2,n}^-(\omega) = \frac{1}{\omega} \left[ \frac{\pi}{2} + 2n\pi + \cos^{-1}(B) \right], \end{cases} \quad (13)$$

where

$$A = A(\omega) = \frac{\omega^2 + s^2\alpha^2 - \delta^2}{2s\alpha\omega}, \quad B = B(\omega) = \frac{\omega^2 - s^2\alpha^2 + \delta^2}{2\delta\omega} > 0.$$

Furthermore, noticing that  $\cos^{-1}(A), \cos^{-1}(B) \in [0, \pi]$ , one has  $\omega\tau_1^+, \omega\tau_2^+ \in [-\pi/2, \pi/2]$  with  $m = n = 0$ .

**Theorem 2** *Let  $n$  be fixed. Then the segments of  $C^+(m, n)$  and  $C^-(m, n)$  form a continuous curve as  $m$  increases.*

**Proof.** In order to understand the possible configurations of stability crossing curves of our model, we analyze the behavior of  $C^+(m, n)$  and  $C^-(m, n)$  at the initial and end points of  $\Omega$ . Since

$$\theta_1(-s\alpha + \delta) = \cos^{-1}(-1) = \pi, \quad \theta_2(-s\alpha + \delta) = \cos^{-1}(1) = 0$$

and

$$\theta_1(s\alpha + \delta) = \cos^{-1}(1) = 0, \quad \theta_2(s\alpha + \delta) = \cos^{-1}(1) = 0,$$

(12) gives that the initial and end points of  $C^+(m, n)$  are

$$I^+(m, n) = \left( \frac{1}{-s\alpha + \delta} \left( \frac{3\pi}{2} + (2m-1)\pi \right), \frac{1}{-s\alpha + \delta} \left( \frac{3\pi}{2} + (2n-1)\pi \right) \right)$$

and

$$E^+(m, n) = \left( \frac{1}{s\alpha + \delta} \left( \frac{\pi}{2} + (2m-1)\pi \right), \frac{1}{s\alpha + \delta} \left( \frac{3\pi}{2} + (2n-1)\pi \right) \right).$$

As well, it follows from (13) that the initial and end points of  $C^-(m, n)$  are

$$I^-(m, n) = \left( \frac{1}{-s\alpha + \delta} \left( \frac{\pi}{2} + (2m-1)\pi - \pi \right), \frac{1}{-s\alpha + \delta} \left( \frac{3\pi}{2} + (2n-1)\pi \right) \right)$$

and

$$E^-(m, n) = \left( \frac{1}{s\alpha + \delta} \left( \frac{\pi}{2} + (2m-1)\pi \right), \frac{1}{s\alpha + \delta} \left( \frac{3\pi}{2} + (2n-1)\pi \right) \right).$$

Since  $I^+(m, n) = I^-(m+1, n)$  and  $E^+(m, n) = E^-(m, n)$ , we arrive at the conclusion that the curves  $C^+(m, n)$  and  $C^-(m, n)$  are connected at the endpoint of  $\Omega$ , while  $C^+(m, n)$  and  $C^-(m+1, n)$  are connected at the initial point of  $\Omega$ . ■

After having determined the stability crossing curves corresponding to  $\Omega$ , we will discuss the direction in which the solutions of (7) cross the imaginary axis as  $(\tau_1, \tau_2)$  deviates from a curve in  $T$  and find the directions of crossing as one moves along the curve.

For discussing the direction of crossing, we need some definitions. We call the direction of the stability switch curve with increasing  $\omega$  the *positive direction*, while the region on the left hand side, as we head in the positive direction of the curve, is called the *region on the left*, denoted by **L**. The region on the right hand side is called the *region on the right*, denoted as **R**.

Gu et al. (2005) proved (see Proposition 6.1) that if  $\lambda = i\omega$  is a simple solution of equation (7), as  $(\tau_1, \tau_2)$  moves from **R** to **L** of the corresponding curve in  $\mathcal{T}$ , then a pair of solutions of (7) cross the imaginary axis to the right if  $Q > 0$ , where

$$Q = \text{Im} \left[ a_1(i\omega)a_2(-i\omega)e^{i\omega(\tau_2-\tau_1)} \right], \quad (14)$$

and the crossing is in the opposite direction if  $Q < 0$ .

**Theorem 3** *As  $(\tau_1, \tau_2)$  moves from **R** to **L**, we have*

- 1) *a stability loss if  $\omega < \delta - s\alpha$  on  $C^+(m, n)$  or if  $\omega > \delta - s\alpha$  on  $C^-(m, n)$ ;*

2) a stability gain if  $\omega > \delta - s\alpha$  on  $C^+(m, n)$  or if  $\omega < \delta - s\alpha$  on  $C^-(m, n)$ .

**Proof.** In the first part of the proof we show by contradiction that the root  $\lambda = i\omega$  is simple. Suppose  $\lambda = i\omega$  is a root of (7) which is repeated. Then, the derivative of (7) with respect to  $\lambda$  evaluated at  $\lambda = i\omega$  must also be zero, and we have the following two equations

$$\begin{cases} i\omega - s\alpha e^{-i\omega\tau_1} + \delta e^{-i\omega\tau_2} = 0, \\ 1 + s\alpha\tau_1 e^{-i\omega\tau_1} - \delta\tau_2 e^{-i\omega\tau_2} = 0. \end{cases} \quad (15)$$

From (15), we get

$$e^{-i\omega\tau_1} = \frac{1 + i\omega\tau_2}{s\alpha(\tau_2 - \tau_1)}, \quad e^{-i\omega\tau_2} = \frac{1 + i\omega\tau_1}{\delta(\tau_2 - \tau_1)}. \quad (16)$$

Separating real and imaginary parts in (16), and then comparing, we obtain

$$\sin \omega\tau_1 = -\omega\tau_2 \cos \omega\tau_1, \quad \sin \omega\tau_2 = -\omega\tau_1 \cos \omega\tau_2.$$

Consequently,

$$\tan \omega\tau_1 = -\omega\tau_2, \quad \tan \omega\tau_2 = -\omega\tau_1. \quad (17)$$

If we are on  $C^+(m, n)$ , we notice from (12) that, being  $\cos^{-1}(A), \cos^{-1}(B) \in [0, \pi]$ , one has that with  $m = n = 0$ ,  $\omega\tau_1^+, \omega\tau_2^+ \in [-\pi/2, \pi/2]$ . Using (17), and recalling that the tangent function is an odd function, we arrive at the identity

$$\tan \omega\tau_1^+ = \tan^{-1} \omega\tau_1^+.$$

On the other hand, a graphical inspection shows that these two functions do not have nonzero intersection when  $\omega\tau_1^+ \in (-\pi/2, \pi/2)$ . The proof when we are on  $C^-(m, n)$  is similar. In conclusion, we have shown that the root  $\lambda = i\omega$  is simple. In this second part of the proof we find the conditions for  $Q > 0$  (stability loss) and for  $Q < 0$  (stability gain). From (14), we have

$$Q = \text{Im} \left\{ -\frac{s\alpha\delta}{\omega^2} [\cos \omega(\tau_2 - \tau_1) + i \sin \omega(\tau_2 - \tau_1)] \right\} = -\frac{s\alpha\delta}{\omega^2} \sin \omega(\tau_2^+ - \tau_1^+). \quad (18)$$

On  $C^+(m, n)$ , it is

$$\omega(\tau_2^+ - \tau_1^+) = [2(n - m) + 1] \pi - [\cos^{-1}(A) + \cos^{-1}(B)]. \quad (19)$$

Therefore, from (18) and (19), using the angle-sum and angle-difference identities for trigonometric functions, i.e.  $\sin(u \pm v) = \sin u \cos v \pm \cos u \sin v$  and  $\cos(u \pm v) = \cos u \cos v \mp \sin u \sin v$ , it follows

$$Q = -\frac{s\alpha\delta}{\omega^2} \sin [\cos^{-1}(A) + \cos^{-1}(B)] = \frac{s\alpha\delta}{\omega^2} \left\{ -B\sqrt{1 - A^2} - A\sqrt{1 - B^2} \right\}.$$

On  $C^+(m, n)$ , one has

$$\text{sign}(Q) = \text{sign} \left( -B\sqrt{1 - A^2} - A\sqrt{1 - B^2} \right).$$

Since  $B > 0$ , and so  $-B < 0$ , we see that  $Q < 0$  if  $A \geq 0$ , i.e. if  $\omega \geq \sqrt{\delta^2 - s^2\alpha^2}$ . Let  $A < 0$ , i.e.  $\omega < \sqrt{\delta^2 - s^2\alpha^2}$ . Then  $Q < 0$  if  $B > -A$ , i.e. if  $\omega > \delta - s\alpha$ . Since  $\sqrt{\delta^2 - s^2\alpha^2} > \delta - s\alpha$ , we have that  $Q < 0$  if  $\omega > \delta - s\alpha$ . As well, we have that  $Q > 0$  for  $\omega < \delta - s\alpha$ .

Similarly, on  $C^-(m, n)$ , one has

$$\omega(\tau_2^- - \tau_1^-) = [2(n - m) + 1] \pi + [\cos^{-1}(A) + \cos^{-1}(B)],$$

yielding

$$Q = \frac{s\alpha\delta}{\omega^2} \sin[\cos^{-1}(A) + \cos^{-1}(B)] = \frac{s\alpha\delta}{\omega^2} \left\{ B\sqrt{1 - A^2} + A\sqrt{1 - B^2} \right\}.$$

Hence,

$$\text{sign}(Q) = \text{sign}\left(B\sqrt{1 - A^2} + A\sqrt{1 - B^2}\right) \text{ on } C^-(m, n).$$

Proceeding as before, we derive  $Q < 0$  if  $\omega < \delta - s\alpha$  and  $Q > 0$  if  $\omega > \delta - s\alpha$ . ■

## 4 Numerical Simulations

We numerically justify the validity of the analytical results obtained in Section 3. To this end, we adopt the Cobb-Douglas production function,

$$f(k) = Ak^\beta$$

with  $\beta \in (0, 1)$  and  $A = 1$ . Since the stationary per capita  $k^*$  solves  $s(k^*)^\beta = \delta k^*$ , the marginal product at the stationary point satisfies the following relation,

$$\beta(k^*)^{\beta-1} = \frac{\beta\delta}{s} (= \alpha)$$

leading to  $s\alpha = \beta\delta$ .

In the first numerical example, we specify the parameter values as follows:

$$s = 0.3, \beta = 0.5 \text{ and } \delta = 0.1.$$

Figure 1(A) shows the stability switching curve in which the red segments are described by  $C^-(m, 0)$  for  $m = 1, 2, 3, 4$  and the left most blue segment by  $C^+(0, 0)$  and the other blue segments by  $C^+(m, 0)$  for  $m = 1, 2, 3$ . Notice that  $m$  is a horizontal-shift parameter and  $n$  is a vertical-shift parameter. The curve divides the non-negative  $(\tau_1, \tau_2)$  plane into two regions. The stationary point is stable in the region including the origin<sup>4</sup> and unstable in the other region. We immediately observe the two results given in Proposition 1 and in the first half of Theorem 3 of Bianca et al. (2013).

- (1) The stationary point  $k^*$  is always stable for  $\tau_2 = 0$  because it is locally asymptotically stable for  $\tau_1 = 0$  and no stability switch occurs for any  $\tau_1 > 0$  as the stability switching curve does not intersect the horizontal axis. These are also shown in Lemma 2.
- (2) For  $\tau_1 = 0$ , the stationary point is locally asymptotically stable for  $\tau_2 < \tau_2^0$ , loses stability at  $\tau_2 = \tau_2^0$  and unstable for  $\tau_2 > \tau_2^0$  where  $\tau_2^0 \simeq 12.09$  is the intersection of the most left blue curve with the vertical axis as shown in Figure 2(A). Lemma 1 formally proves this observation.<sup>5</sup>

<sup>4</sup>We have already confirmed that  $k^*$  is stable in case of no delays (i.e.,  $\tau_1 = \tau_2 = 0$ ).

<sup>5</sup>The critical value  $\tau_2^0$  is identical with  $\tau_2^*$  obtained in Lemma 1. Hence

$$\tau_2^0 = \frac{1}{\delta\sqrt{1 - \beta^2}} \sin^{-1}\left(\sqrt{1 - \beta^2}\right) = \frac{20\pi}{3\sqrt{3}} \simeq 12.09$$

where  $\alpha s = \beta\delta$  is used to simplify the form of  $\tau_2^0$ .

We can obtain more results. First, notice that since the blue curves take  $U$ -shaped form, it has a minimum value denoted by  $\tau_2^m \simeq 9.35$ , which is obtained by differentiating  $\tau_{2,m}(\omega)$  with respect to  $\omega$  and solving the resultant expression being equal to zero.

- (3) For  $\tau_2 < \tau_2^m$ , any  $\tau_1 \geq 0$  is harmless implying that the equilibrium point is locally asymptotically stable. The destabilizing effect caused by the depreciation delay is thought to be dominated by the stabilizing effect by the gestation delay.
- (4) The upward sloping solid black line is the locus of  $\tau_1 = \tau_2$  (i.e., diagonal) and passes through the connecting point of  $I^+(0, 0)$  and  $I^-(1, 0)$  where

$$I^+(0, 0) = I^-(1, 0) = \left\{ \frac{\pi}{2(\delta - \alpha s)}, \frac{\pi}{2(\delta - \alpha s)} \right\}.$$

Notice that the both elements are the same and equivalent to  $\tau^*$  obtained in Lemma 3. For asymmetric pair of  $(\tau_1, \tau_2)$  in a small neighborhood around the diagonal, the resultant dynamics could be similar to that with a pair on the diagonal.

We now turn attention to Figure 1(B) that is an enlargement of the shaded rectangular region in Figure 1(A). According to Theorem 2, both  $C^+(0, 0)$  and  $C^-(1, 0)$  start but in the opposite direction at the green point where  $I^+(0, 0) = I^-(1, 0)$  holds and both  $C^+(1, 0)$  and  $C^-(1, 0)$  finally arrive at the yellow point where  $E^+(1, 0) = E^-(1, 0)$  holds. As shown by arrows, the point of  $(\tau_1, \tau_2)$  on the red curve moves from the green point to the yellow point as the value of  $\omega$  increases. By the same token, the point on the lower blue curve moves forward to the yellow point and the point on the upper blue curve moves away from the yellow point as the value of  $\omega$  increases. As seen in Figure 1(B), the vertical line standing at  $\bar{\tau}_1 = (\tau_1^m + \tau_1^M)/2$  crosses the stability switching curve three time at points  $a, b$  and  $c$  where  $\tau_1^m \simeq 29.8$  and  $\tau_1^M \simeq 40.57$  are the minimum and maximum values of  $\tau$  along the inverse  $S$ -shaped red curve. The  $\tau_2$ -value of point  $a$  is calculated as follows. Solving  $\tau_{1,1}^+(\omega) = \bar{\tau}_1$  gives  $\omega_a \simeq 0.145$  that is, in turn, substituted into  $\tau_{2,0}^-(\omega)$  to determine  $\tau_2^a \simeq 9.56$ . In the same way, we have  $\omega_b \simeq 0.092$  and  $\tau_2^b \simeq 22.63$  at point  $b$  and  $\omega_c \simeq 0.051$  and  $\tau_2^c \simeq 33.14$  at point  $c$ . At each point, the stability switch occurs according to Theorem 3:

- (5-a) Since the lower blue curve is described by  $C^+(1, 0)$  and passes through point  $a$  from right to left in the positive direction, the **R**-region is above the curve and the **L**-region is below. The specified values of the parameters lead to  $\delta - s\alpha = \delta - \beta\delta = 0.05 < \omega_a$ , the value of  $\omega$  at point  $a$ . Theorem 2 (1) implies that as  $(\tau_1, \tau_2)$  moves downward from **R** to **L** along the vertical line passing through point  $a$ , the stability is gained.
- (5-b) The red curve is described by  $C^-(1, 0)$ . With the positive direction in the neighborhood of point  $b$ , the pair of the delay moves right to left along the downward part of the red curve as the arrows exhibit. The **R**-region is above the curve and the **L**-region is below. Hence, as in the same way as above, Theorem 2 (1) indicates that the stability is lost when the pair of the delays moves downward from **R** to **L** along the vertical line passing through point  $b$  at which  $\omega_b > \delta - s\alpha$  on  $C^-(1, 0)$ .
- (5-c) The positive direction is reversed in the neighborhood of point  $c$  so that the **R**-region is below the positive sloping part of the red curve and the **L**-region is above. Theorem 3 (1) also indicates that the stability is lost when the pair of the delay moves upward from **R** to **L** along the vertical line passing through point  $c$  at which  $\omega_c > \delta - s\alpha$  on  $C^-(1, 0)$ .

The last results are summarized as follows: when the value of  $\tau_2$  increases along the vertical line at  $\bar{\tau}_1 \in (\tau_1^m, \tau_1^M)$ , the switch from stability to instability occurs at the first intersection, the stability is regained at the second intersection and the stability is lost again at the third intersection. No stability switch occurs for further increase of  $\tau_2$ .

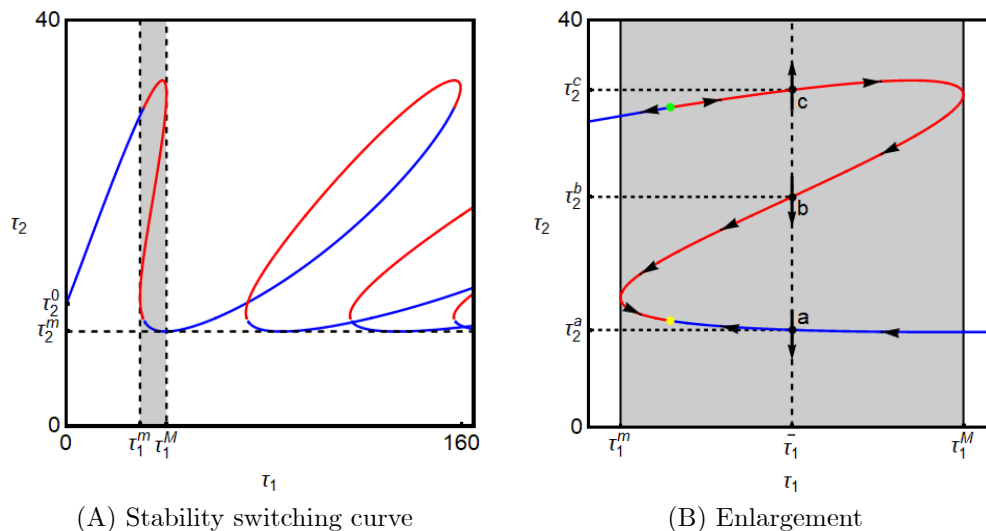


Figure 2. Stability switching curve

The dynamic results we have obtained so far concern local dynamics. To examine global dynamics, we perform numerical simulations. Figure 3 is a bifurcation diagram of two delay model with respect to  $\tau_2$  along the vertical line at  $\bar{\tau}$  in Figure 2(B). It has been proved that the stationary point loses stability at  $\tau_2^a$  and  $\tau_2^c$  and gains stability at  $\tau_2^b$  and these theoretical results are numerically confirmed in Figure 3 where the red curves describe trajectories of  $k(t)$  for  $t \in [8, 35]$ . It is further seen that a Hopf cycle appears just after  $\tau_2$  passes through  $\tau_2^a$  and just before  $\tau_2$  arrives at  $\tau_2^c$ . It follows from this bifurcation diagram, the trajectories become negative and loses its economic meaning for most values  $\tau_2$  in the unstable interval  $[\tau_2^a, \tau_2^b]$ . It can be supposed that the unstable depreciation delay effect becomes rapidly larger than the stable gestation delay effect. It is also

observed that an economically meaningful limit cycle appears for  $\tau_2$  larger than  $\tau_2^c$ .

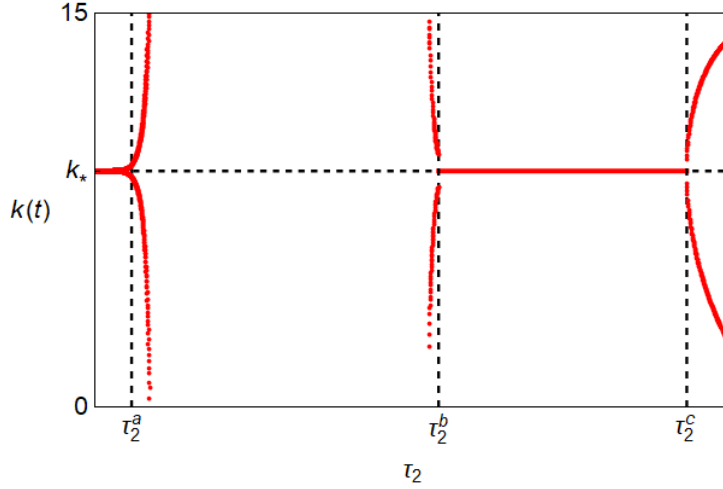


Figure 3. Bifurcation diagram

We now visit the numerical examples considered by Bianca et al. (2013) and confirm their results in our way. We start to examine their first and second examples together, both of which have the same parameter values

$$s = 0.11, \beta = 0.1 \text{ and } \delta = 0.8$$

and two sets of the delay combination  $(\tau_1, \tau_2)$ ,

$$A = (1, 2) \text{ and } B = (3, 2)$$

where point  $A$  represents a case of  $\tau_1 < \tau_2$  and so does point  $B$  a case of  $\tau_1 > \tau_2$ . The stability switching curve is illustrated in Figure 4(A) in which the solid blue and red curves are described by  $C^+(m, 0)$  and  $C^-(m, 0)$  for  $m = 1, 2$ . Let us examine dynamics at point  $A$ . For  $\tau_1 = 1$ , we can calculate the corresponding value of  $\tau_2$  to be on the stability switching curve by two steps. At the first step we solve  $\tau_{1,0}^+(\omega) = 1$  to obtain  $\omega_1 \simeq 0.744$ . At the second step this  $\omega_1$  is substituted into  $\tau_{1,0}^-(\omega_1) \simeq 2.013$ . Hence, this threshold value is slightly larger than 2. Point  $A$  is below the stability switching curve and thus time trajectories under the  $A$ -specification converge to the stationary point. We now turn attention to point  $B$ . Without any calculations, it is apparent that point  $B$  is located below the stability switching curve and thus the stationary point is also locally asymptotically stable under the  $B$ -specification. Using the stability switching curve, we can confirm that the model with either the  $A$ -specification or the  $B$ -specification is locally asymptotically stable without performing numerical simulations. They also numerically show that stability is sensitive to the selection of the value of  $\beta$ . It is shown that stability under  $\beta = 0.1$  is lost when the value is decreased to  $\beta = 0.01$ . We illustrate the stability switching curve under  $\beta = 0.01$  as the dotted blue and red curve in Figure 4(A) and find that points  $A$  and  $B$  are above the dotted curve, implying instability.

We have two more results. One is that  $\tau_1$  becomes harmless when  $\tau_2 < \tau_2^m \simeq 1.751$  and the other is that stability loss and gain can occur repeatedly as the stability switching curve is wave-shaped. In particular, when the value of  $\tau_1$  is increased along the horizontal line at  $\tau_2 = 2$ , the stability is gained whenever the horizontal line crosses the positive sloping blue curve whereas the stability is lost whenever the horizontal line crosses the negative sloping red curve. Although we do not provide a bifurcation diagram obtained under these new parameter specification, it is confirmed first that a Hopf bifurcation can occur when stability is lost and second that economically meaningful cycles are obtained only a very small interval of time delay as shown in Figure 3.

In their third example, the parameter values are changed to

$$s = 0.41, \alpha = 0.8 \text{ and } \delta = 0.35$$

and the combination of delays is selected as

$$C = (10, 2).$$

The corresponding stability switching curves are illustrated by the blue curve and blue-red curve in Figure 4(B). For  $\tau_1 = 10$ , the corresponding  $\tau_2$ -value of  $C^+(1, 0)$  is approximately 2.018, slightly larger than 2. Therefore point  $C$  is actually located in the stable region below the stability switching curve. In consequence, although it takes much longer time to arrive at the equilibrium point, as point  $C$  is very close to the switching curve, the equilibrium point is locally asymptotically stable, oscillations can occur for a long time. In this example, the multiple stability loss and gain can occur. In fact, if we increase the value of  $\tau_2$  along the dotted vertical line at  $\tau_1 = 10$ , we have three intersections, stability is lost at the first intersection at  $\tau_2 \simeq 2.018$ , regained at crossing point  $a$  with the red curve  $\tau_2^a \simeq 6.676$  and finally lost again at crossing point  $b$  with the upper blue curve,  $\tau_2^b \simeq 11.868$ .

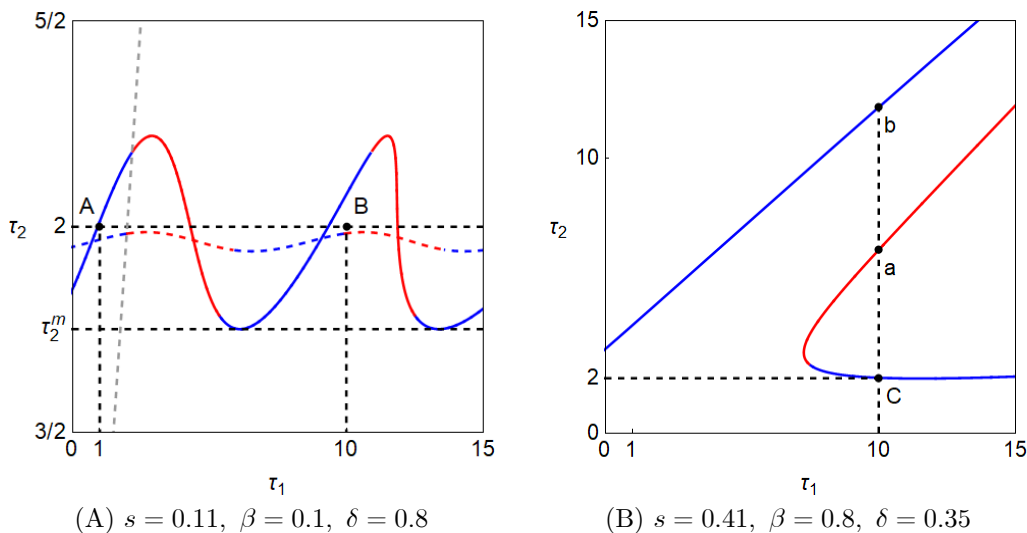


Figure 4. Stability switching curves in examples of Bianca et al. (2013)



## 5 Concluding Remarks

Stability of the traditional neoclassical model was examined under the assumption that there were two distinct delays, one is the gestation or production delay and the other is the depreciation delay. Confirming that the no delay version was locally asymptotically stable, we demonstrated analytically and numerically that it could generate qualitatively different dynamics once one or two delays were introduced:

- (1) In one delay version, the gestation delay has a stabilizing effect and the depreciation delay has a destabilizing effect, implying that the model with the gestation delay was always locally asymptotically stable and the stability of the model with the two but equal delays depends on the relative magnitude of the opposite effects.
- (2) In two delays version, stability switching curves were constructed in Theorem 2 and stability loss and gain on the stability switching were confirmed in Theorem 3.
- (3) In numerical version with two delays, we have several results:
  - (3-a) the stability switching curve can take a wave-shape, implying multiple occurrence of stability loss and gain;
  - (3-b) there is a threshold value of the depreciation delay (i.e.,  $\tau_2^m$ ), the stationary point is locally asymptotically stable if  $\tau_2 < \tau_2^m$ , regardless of a value of  $\tau_1$ ;
  - (3-c) although the existence of a Hopf cycle is confirmed, it depends on the parameter specification whether a resultant cycle is economically meaningful.

One possible direction of extending our study is to introduce delays into the optimal growth model. Asea and Zak (1999) and Zak (1999) present partial results that should be improved. The other possible direction is to consider a two-sector growth model with multiple delays. Furuno (1965) shows the existence of a cycle under the Leontief type production function. It is interesting to examine the same issue under the neoclassical production function and two delays.

## References

- [1] Asea, P. K., and Zak, P. Time to build and cycles, *Journal of Economic Dynamics and Control*, 23, 1155-1175, 1999.
- [2] Bianca, C., Ferrara, M. and Guerrini, L., The time delays' effects on the qualitative behavior of an economic growth model, *Abstract and Applied Analysis*, 2013, Article ID 901014, 10 pages, <http://dx.doi.org/10.1155/2013/901014>.
- [3] Day, R., Irregular growth cycle, *American Economic Review*, 72, 406-414, 1982.
- [4] Furuno, Y., The period of production in two-sector model of economic growth, *International Economic Review*, 6, 240-244, 1965.
- [5] Gu, K., Niculescu, S. and Chen, J., On stability crossing curves for general systems with two delays. *Journal of Mathematic Analysis and Application*, 311, 231-252, 2005.
- [6] Kalecki, M., A macrodynamic theory of business cycles, *Econometrica*, 3, 327-344, 1935.
- [7] Kydland, F. E. and Prescott, E., Time to build and aggregate fluctuations, *Econometrica*, 50, 1345-1370, 1982.
- [8] Matsumoto, A. and Szidarovszky, F., An elementary study of a class of dynamic system with single delay, *CUBO A MATHematical Journal*, 15, 1-7, 2013.
- [9] Matsumoto, A. and Szidarovszky, F., Nonlinear delay monopoly with bounded rationality, *Chaos, Solitons and Fractals*, 45, 507-519, 2012.
- [10] Matsumoto, A. and Szidarovszky, F., Delay differential neoclassical growth model, *Journal of Economic Behavior and Organization*, 78, 272-289, 2011.
- [11] Solow, R., A contribution to the theory of economic growth, *Quarterly Journal of Economics*, 70, 65-94, 1956.
- [12] Swan, T., Economic growth and capital accumulation, *Economic Record*, 32, 334-361, 1956.
- [13] Szydłowski, M. and Krawiec, A., A note on Kaleckian lags in the Solow model, *Review of Political Economy*, 16, 5-1-506, 2004.
- [14] Zak, P., Kaleckian lags in general equilibrium, *Review of Political Economy*, 11, 321-330, 1999.